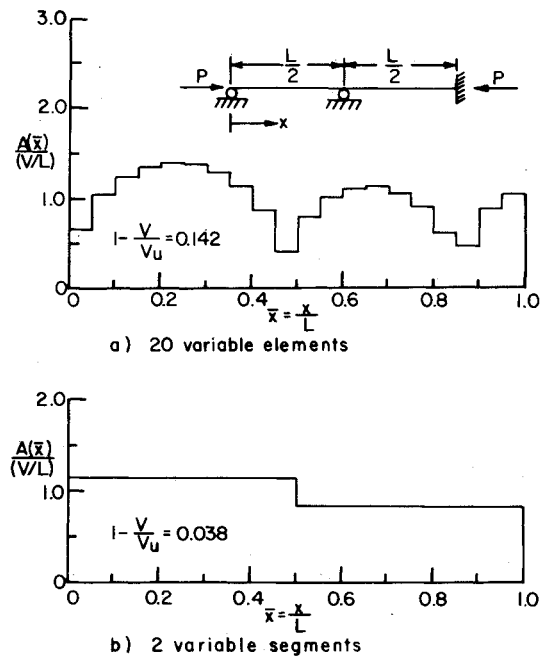

Fig. 2 Optimum shape of a continuous beam.

V_u is the volume of the uniform column having the same buckling load. The savings in weight over a uniform column of equal buckling strength is 12.8% with the present method compared with 14.0% obtained from the analytical solution. The initial design was taken as a uniform column having a buckling strength equal to 10% of the prescribed value; using a CDC 6600, CP time was 23 sec.

Example b

The second example is a continuous column having hinged-clamped outer supports and a roller at midspan. Considering the axial force to be constant, and taking the same weight-stiffness relationship as in the previous example, the optimal material distribution is as indicated in Fig. 2. The results of allowing each of the 20 elements to vary independently is shown in Fig. 2a. The savings in weight over a uniform column of equal strength is 14.2%. By forcing all the elements in each span to maintain the same cross section, the volume distribution is that shown in Fig. 2b; the material savings is 3.8%. It should be mentioned that if the structure were represented by only one element per span, the model would lead to large inaccuracies. The buckling load for such a model, e.g., is 28.9% in excess of the exact value; subsequent optimization would, therefore, incorrectly imply a material savings of 36.8%, which represents a large unconservative error.

References

[1] Zarghamee, M. S., "Optimum Frequency of Structures," *AIAA Journal*, Vol. 6, No. 4, April 1968, pp. 749–750.

[2] Rubin, C. P., "Minimum Weight Design of Complex Structures Subject to a Frequency Constraint," *AIAA Journal*, Vol. 8, No. 5, May 1970, pp. 923–927.

[3] Sheu, C. Y. and Prager, W., "Minimum Weight Design with Piecewise Constant Specific Stiffness," *Journal of Optimization Theory and Applications*, Vol. 2, No. 3, March 1968, pp. 179–186.

[4] Chern, J. M. and Prager, W., "Optimal Design of Beams for Prescribed Compliance Under Alternate Loads," *Journal of Optimization Theory and Applications*, Vol. 5, No. 6, June 1970, pp. 425–431.

[5] Tadjbakhsh, I. and Keller, J. B., "Strongest Columns and Isoperimetric Inequalities for Eigenvalues," *Journal of Applied Mechanics*, Vol. 29, No. 1, March 1962, pp. 159–164.

Reflectance and Unsteady Temperature Distribution of Diffuse Reflectors

KENNETH C. WESTON* AND R. S. REDDY†
University of Tulsa, Tulsa, Okla.

THE applicability of the Kubelka-Munk two flux approach to the estimation of the temperature distribution in volume reflectors was pointed out in Ref. 1. There an historic exact solution of the Kubelka-Munk equations for the reflectance of an absorbing and scattering material was presented. A reflectance solution of the Kubelka-Munk equations for the case of zero absorption coefficient was also presented and applied to the problem of the calculation of steady-state temperature distributions in volume reflectors. The adequacy of the zero absorption coefficient solution for the approximation of the reflectance of a weakly absorbing, highly scattering material is considered here. A solution for the transient heating of a one-dimensional volume reflector is given. The effect of the error incurred in employing the zero absorption equation for the estimation of the transient heating of a volume reflector is then considered for early times appropriate to the entry heat protection system application.

Reflectance solutions of the Kubelka-Munk differential equations are expressed in terms of the ratio of absorption to scattering coefficient, k/s, the scattering power, $S = s\delta$, and the rear surface reflectance, R_B, where δ is the thickness of the one-dimensional volume reflector. The reflectance of a diffuser of infinite thickness is given by

$$R_\infty = 1 + k/s - [k/s(k/s+2)]^{1/2} \tag{1}$$

The reflectance of a thickness δ of this material backed with a material of reflectance R_B is then expressed in terms of R_∞ as

$$R = \frac{(1/R_\infty)(R_B - R_\infty) - R_\infty(R_B - 1/R_\infty)\exp[S(1/R_\infty - R_\infty)]}{(R_B - R_\infty) - (R_B - 1/R_\infty)\exp[S(1/R_\infty - R_\infty)]} \tag{2}$$

A solution of the Kubelka-Munk equations for $k = 0$ is also available:

$$R_{k=0} = [1-(1-R_B)(1-S)]/[1+(1-R_B)S] \tag{3}$$

These reflectance solutions are exact solutions of the Kubelka-Munk differential equations. The relative simplicity of Eq. (3) suggests that it may be more convenient to apply this equation as an approximation for weakly absorbing materials than Eq. (2). Such an application was made in Refs. 1 and 2. These solutions assume that internal emission is negligible for the weak absorption, moderate temperature conditions presumed here.

A comparison of Eqs. (2) and (3) is given in Fig. 1 for the case of $R_B = 0.95$ and a range of values of k/s and S. For the case of S approaching zero, the over-all reflectance tends towards the reflectance of the rear surface. For small values of k/s, it is evident that Eq. (2) indicates that increasing the scattering power increases the over-all reflectance due to the dominance of the scattering centers within the material. For values of k/s exceeding about 10^{-3}, it is seen that the reflectance falls below the back surface reflectance due to dominance of absorption processes within the material.

Of primary interest here are extremely low values of k/s which are characteristic of good diffuse reflectors. It is seen in Fig. 1 that the nonabsorbing solution given in Eq. (3) approximates, for these low k/s values, the reflectance of diffuse reflectors as characterized by Eq. (2). As an example, values of k and s have been estimated for fritted quartz in Ref. 2 to be $k = 0.005$ cm^{-1} and $s = 10$ cm^{-1}. For these values and a

Received May 31, 1973. This research has been partially supported under NASA Grant NGR 37-008-003.

Index categories: Entry Vehicles and Landers; Heat Conduction; Radiation and Radiative Heat Transfer.

* Associate Professor of Mechanical Engineering. Member AIAA.
† Graduate Research Assistant.

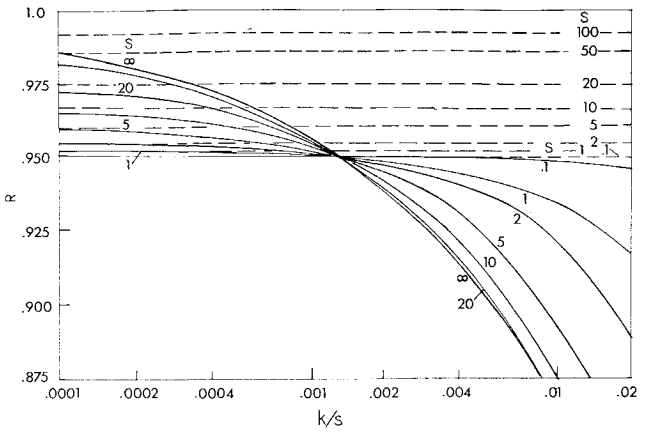

Fig. 1 Diffuse reflectance of a material with internal scattering. $R_B = 0.95$. Solid lines—Eq. (2). Dashed lines—Eq. (3).

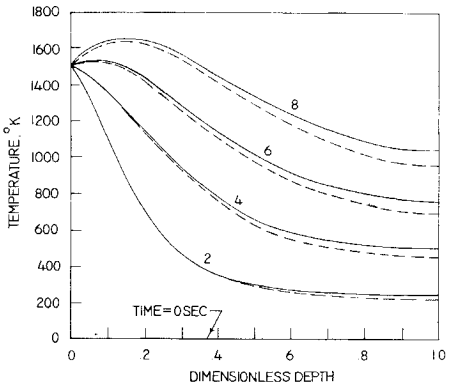

Fig. 3 Estimated unsteady temperature distributions in 1 cm thickness of quartz. $R_B = 0.95$, $T_2 = 0°K$, $T_1 = 1500°K$, $q_0 = 50$ kw/cm^2, $s = 10$ cm^{-1}, $k = 0.005$ cm^{-1}, $\rho = 2.5$ g/cm^3, $C = 1.15$ w-sec/g°K, $K = 0.0251$ w/cm°K. Solid lines—Eq. (3). Dashed lines—Eq. (2).

thickness of 1 cm, Eq. (2) yields a value of $R = 0.961$ while the zero-absorption Eq. (3) yields $R = 0.967$, an error of less than 1%. While $R = 0.961$ represents a small increase over the 0.95 back surface reflectance, the over-all reflectance of this configuration is primarily attributable to the scattering processes. This is easily verified by calculation of the reflectance of the configuration with zero back surface reflectance. The resulting value, $R = 0.906$, indicates little contribution of the high back surface reflectance of the original configuration to the over-all reflectance. The influence of back surface reflectance on the over-all reflectance for good and poor volume reflecting materials is illustrated in Fig. 2. It is evident that for good volume reflecting materials, the back surface reflectance is important only for small material thicknesses. Thus in an entry heat protection system application the back surface reflectance may become increasingly important as sublimation of front surface material proceeds.

The influence of reflectance error on the internal temperature of a volume reflector may be evaluated by considering the initial boundary value problem in which a volume reflecting material, initially at a constant temperature T_2, is exposed at time zero to a step increase in temperature, $T_1 - T_2$, at one boundary ($y = 0$) and to a uniform, incident, diffuse radiative flux, q_0, through that boundary. The interaction of the temperature and the radiation field is represented by the radiative heat flux divergence term

$$dq_R/dy = -kq_0[1 + R - 2sy(1-R)] \tag{4}$$

developed in Ref. 1, from the approximate Kubelka-Munk model for weakly absorbing materials. The boundary condition at the back surface ($y = \delta$) is taken to be adiabatic. Thus the initial boundary value problem may be stated

$$\rho C\, \partial T/\partial t = K\, \partial^2 T/\partial y^2 + kq_0[1 + R - 2sy(1-R)] \tag{5a}$$

$$T(0,t) = T_1, \quad T_y(\delta, t) = 0 \qquad t > 0 \tag{5b, c}$$

$$T(y,0) = T_2 \qquad 0 \leqq y \leqq \delta \tag{5d}$$

where K, ρ, and C are the thermal conductivity, density, and heat capacity of the material. Defining the following dimensionless parameters:

$$\tau = Kt/\rho C\, \delta^2, \quad \eta = y/\delta, \quad \theta = T/T_s, \quad \phi = kq_0\delta^2/KT_s$$

where T_s is an arbitrarily selected reference temperature, the problem (5) may be given in nondimensional terms as

$$\partial\theta/\partial\tau = \partial^2\theta/\partial\eta^2 + \phi_R(\eta) \tag{6a}$$

$$\theta(0,\tau) = \theta_1, \quad \theta_\eta(1,\tau) = 0 \qquad \tau > 0 \tag{6b, c}$$

$$\theta(\eta, 0) = \theta_2 \qquad 0 \leqq \eta \leqq 1 \tag{6d}$$

where

$$\phi_R(\eta) = \phi[1 + R - 2S\eta(1-R)] \tag{7}$$

The solution of Eq. (6) may be obtained by solution for the steady-state and transient parts,[3] resulting in

$$\theta(\eta,\tau) = \theta_1 + \phi\left\{[1 + R - S(1-R)]\eta - \frac{1+R}{2}\eta^2 + S(1-R)\frac{\eta^3}{3}\right\} + 2\phi\sum_{n=0}^{\infty}\left[\frac{2S(1-R)}{\lambda_n^2(-1)^n} - \frac{1+R}{\lambda_n^{1.5}} + \frac{\theta_2 - \theta_1}{\phi\lambda_n^{0.5}}\right]e^{-\lambda_n\tau}\sin[(\lambda_n)^{1/2}\eta] \tag{8}$$

where $\lambda_n = (2n+1)^2\pi^2/4$, $n = 0, 1, \ldots$ are the eigenvalues of the related homogeneous problem. The reflectance R in Eq. (8) may be obtained from either Eq. (2) or Eq. (3).

Estimates of the temperature distributions in a quartz slab described above during early phases of intense radiative heating are shown in Fig. 3 based on reflectance values from both Eqs. (2) and (3). It is seen that the small difference in reflectance causes a significant difference in internal temperature. For example at the back surface the temperature difference after 8 sec of heating is 83°K. It should be noted that the use of the higher reflectance obtained from the zero absorption equation leads to higher temperatures. This is a purely numerical result and should not cause confusion with the physical effect of decreasing the temperature through increased scattering or reduced absorption. This physical temperature reduction appears as a combined effect in Eq. (8) of change in s and k as well as in R, rather than the change induced by substitution for R from Eq. (3) instead of (2). Thus care should be exercised in employing Eq. (3) in lieu of Eq. (2) in thermal analyses based on the Kubelka-Munk formalism developed here and in Refs. 1 and 2.

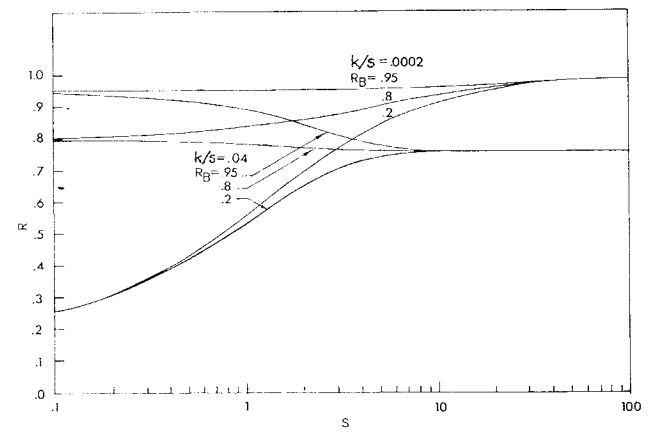

Fig. 2 The transition from low to high scattering power for several values of R_B and k/s.

References

[1] Weston, K. C., Howe, J. T., and Green, M. J., "Approximate Temperature Distribution for a Diffuse, Highly Reflecting Material," *AIAA Journal*, Vol. 10, No. 9, Sept. 1972, pp. 1252–1254.

[2] Howe, J. T., Green, M. J., and Weston, K. C., "Thermal Shielding by Subliming Volume Reflectors in Convective and Intense Radiative Environments," *AIAA Journal*, Vol. 11, No. 7, July 1973, pp. 989–994.
[3] Reddy, R. S., "Approximate Analyses for the Transient Thermal Response of a Weakly Absorbing Medium Undergoing Combined Conductive and Radiative Transfer," Masters thesis, 1973, Univ. of Tulsa, Tulsa, Okla.

Verification of a Simple Relationship for Shock-Wave Reflection in a Relaxing Gas

RONALD K. HANSON* AND WILLIAM FLOWER†
Stanford University, Stanford, Calif.

A SIMPLIFIED description of shock-wave reflection in a relaxing gas was recently presented by Hanson.[1] The theoretical model, which has useful applications to shock-tube studies, is based on the fact that the characteristic relaxation time behind a reflected shock wave is generally much shorter than the corresponding relaxation time behind the preceding incident shock wave. A useful result of the approximate theory is the simple relationship between the time-varying pressure at a shock-tube end wall and the spatially varying density in the incident-shock relaxation zone[1]

$$P(t)/P_{\text{final}} = [\eta(s)-1]/(\eta_{\text{final}}-1)$$

The function η is the spatially varying density ratio ρ/ρ_1, evaluated at the distance s behind the incident shock wave, and t is the time after shock reflection. Thus measurements of pressure can be used to study incident-shock relaxation phenomena, without requiring complex calculations of the shock-reflection process and with significant possible increases in accuracy, operating range and temporal resolution over density measuring techniques.

The pressure measurement technique has already been successfully applied in several studies of vibrational[2,3] and chemical[4,5] kinetics, although the accuracy of the simple relationship between pressure and density has not been confirmed by direct experiment. The present study provides such direct experimental verification in the form of simultaneous measurements of density and pressure in the same shock-wave relaxation experiment.

The experiments were conducted in vibrationally relaxing O_2. The density in the incident-shock relaxation zone was monitored using a quantitative laser-schlieren method similar to that developed by Kiefer and Lutz[6] and described recently by Breshears, Bird, and Kiefer.[7] The method involves measurement of the deflection of a laser beam due to passage of the beam through the relaxing gas behind a shock wave. The relaxation produces an axial density gradient $d\rho/dy$ within the shock tube, and this density gradient causes a beam deflection D at a distance L beyond the shock tube of

$$D = RLw(d\rho/dy)$$

where R is the specific refractivity of the gas (0.19 cm^3/gm for O_2) and w is the internal width of the shock tube.

A schematic of the present arrangement is shown in Fig. 1. The 6328 A beam from a 2 mw helium-neon laser (Spectra-Physics Model 133) is reduced in diameter (to about 0.3 mm) with a simple telescope, and passed through the shock tube in a plane normal to the tube axis. The beam is tilted slightly in the vertical direction to avoid interference between the main beam and components reflected from the window surfaces. Two meters from the center of the tube the beam is divided by a metal-coated prism, and the individual beams are focussed onto matching photodiode detectors (RCA C30808, 2.5-mm-diam active area). The entire optical system is compactly arranged on a single 60 cm × 120 cm vibration-isolated table.

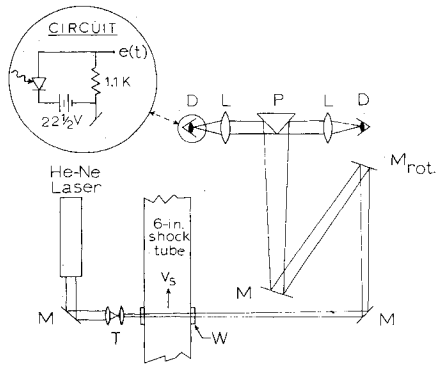

Fig. 1 Laser-schlieren system for incident-shock measurements of density gradient: M = mirror, P = prism (metal-coated), W = window (8 mm dia), L = lens (10-cm focal length), D = photodiode detector, T = telescope (2.7 power).

Deflection of the beam from its initially centered position on the prism apex produces equal and opposite changes in light intensity at the detectors, which are a.c.-coupled to the differential preamplifier of an oscilloscope. Differencing the detector outputs thus provides a signal proportional to beam deflection, but with reduced noise and doubled sensitivity over a single-beam system. For small beam deflections, the voltage displayed on the oscilloscope is linearly proportional to beam deflection and hence also to the density gradient.[6,7] The overall detector circuit-oscilloscope response time (determined by the load resistor and the circuit capacitance to ground) is less than 0.1 μsec (0–63%).

The system was calibrated using a rotating mirror (M_{rot} in Fig. 1) mounted on the shaft of a small electric motor. Knowledge of the rotational speed (3300 rpm) and distance from mirror to prism are sufficient to infer a calibration constant (about 250 mv/mm of deflection at the prism) from an oscillogram. Removal of the telescope from this same optical arrangement results in a reduction in spatial resolution and an increase in sensitivity of about a factor of two.

Results obtained with the laser-schlieren system for an $M = 5.51$ shock wave into O_2 (taken directly from a commercial cylinder, purity greater than 99.99%) are shown in Fig. 2. For comparison,

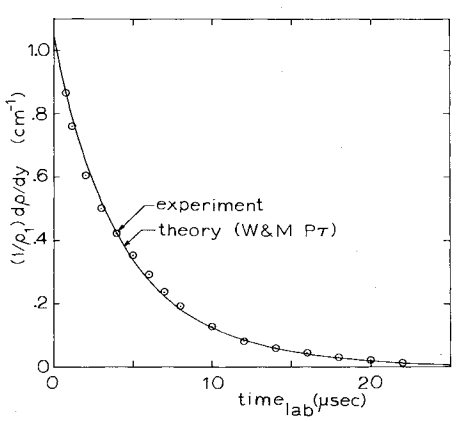

Fig. 2 Reduced record of the density gradient for a shock wave in pure O_2. The experimental conditions were: P_1 = 4.33 torr, V_s = 1.817 mm/μsec, T_1 = 299°K. The solid curve was calculated using the relaxation-time expression of White and Millikan.[8]

Received June 7, 1973. This research was supported by NASA Grant NGR-05-020-583.
Index categories: Reactive Flows; Shock Waves and Detonations.
* Research Associate, Department of Mechanical Engineering.
† NSF Fellow, Department of Mechanical Engineering.